Supplementary Information

Theranostic Metal-Organic Framework Core-Shell Composites for Magnetic Resonance Imaging and Drug Delivery

Huai-Xin Zhao,[‡b] Quan Zou,[‡a] Shao-Kai Sun,[a] Chunshui Yu,[a,c] Xuejun Zhang,[a] Rui-Jun Li,[a] and Yan-Yan Fu[✉a]

[a] School of Medical Imaging, Tianjin Medical University, Tianjin 300203, China.

[b] College of Chemistry, Research Center for Analytical Sciences, State Key Laboratory of Medicinal Chemical Biology (Nankai University), Tianjin Key Laboratory of Molecular Recognition and Biosensing, and Collaborative Innovation Center of Chemical Science and Engineering (Tianjin), Nankai University, 94 Weijin Road, Tianjin 300071, China

[c] Department of Radiology, Tianjin Key Laboratory of Functional Imaging, Tianjin Medical University General Hospital, Tianjin 300052, China.

‡ These authors contributed equally to this work.

✉ Corresponding author. Email: fuyanyan365@163.com

Experimental Section

1. Chemicals and Materials

All chemicals and reagents used were at least of analytical grade. Ultrapure water was purchased from Tianjin Wahaha Group Co., Ltd. Zirconium chloride ($ZrCl_4$) was purchased from J&K Scientific Ltd. (Beijing, China). 2-amino-1,4-benzenedicarboxylate (NH_2-H_2BDC) was purchased from Alfa Aesar. Iron(III) chloride hexahydrate ($FeCl_3 \cdot 6H_2O$), poly(acrylic acid) (PAA, M.W~3000), urea, ethylene glycol and 3-(4,5-dimethylthiazol-2-yl)-2,5-diphenyltetrazolium bromide (MTT) were purchased from Shanghai Aladdin Chemistry Co., Ltd. (Shanghai, China). *N, N*-dimethylformamide (DMF) and dimethyl sulfoxide (DMSO) were purchased from Concord Fine Chemical Research Institute (Tianjin, China). Doxorubicin hydrochloride was purchased from Beijing Huafeng United Technology Co., Ltd. (Beijing, China).

2. Instrumentation and Characterization

Transmission electron microscope (TEM) images were recorded on a JEM-100CXII microscope (JEOL, Japan). High angle annular dark field scanning transmission electron microscope (HAADF-STEM), elemental mapping and EDS (energy dispersive spectrometer) line scanning were performed on FEI Tecnai G2 F20 S-TWIN at 200 kV. X-ray diffraction (XRD) patterns were performed on a D/max-2500 diffractometer (Rigaku, Japan) using $Cu_{K\alpha}$ radiation (λ = 1.5418 Å). The X-ray photoelectron spectroscopy (XPS) spectra were measured on an Axis Ultra DLD (Kratos Analytical Ltd., Britain). Fourier transform infrared (FT-IR) spectra (4000-400 cm^{-1}) were recorded on a Magna-560 spectrometer (Nicolet, Madison, WI, USA) in KBr plates. The UV-vis-NIR absorption spectra were recorded on a UV-3600 spectrophotometer (Shimadzu, Japan). The fluorescence measurements were performed on an F-4500 fluorescence

spectrofluorometer (Hitachi, Japan). Dynamic light scattering (DLS) and zeta potential were carried out on a Malvern Zetasizer (Nano series ZS, Malvern Instruments, UK). Brunauer-Emmett-Teller (BET) surface area, pore volume and pore size distribution were measured on A NOVA 2000e surface area and pore size analyzer (Quantachrome, Florida, FL, USA) using nitrogen adsorption at 77 K in the range $0.02 \leq P/P_0 \leq 0.20$, respectively. The contents of Zr and Fe elements in the prepared Fe_3O_4@UiO-66 composites were measured by an X series inductively coupled plasma mass spectrometer (ICP-MS) (Thermo Elemental, UK) and Atomic Absorption Spectroscopy (AAS, Hitachi 180-80, Japan), respectively. The transverse relaxivity times and T_2-weighted MR images were measured on a MesoMR60 MRI system (Niumag Corporation, Shanghai, China) under the following sequence (multi spin-echo, TR/TE=2000/60 ms, FOV of 100×100 mm, slices=1, matrix of 192×256, 0.55 T, 32.0 °C). The saturation magnetization curve was measured at room temperature on a SQUID VSM from -70 kOe to +70 kOe (Quantum Design, San Diego, USA).

3. Synthesis of Fe_3O_4, Fe_3O_4@UiO-66 and UiO-66 nanoparticles

3.1 Synthesis of Fe_3O_4 nanoparticles. Fe_3O_4 nanoparticles were synthesized according to a literature method with slight modifications.[1] 0.54 g of $FeCl_3 \cdot 6H_2O$ was completely dissolved in 20 mL of ethylene glycol to form a uniform solution under ultrasonic and vigorous stirring. Then, 0.192 g of PAA, 1.5 mL of deionized water, and 1.2 g of urea were successively added. The mixture was ultrasonicated for 10 min and then sealed in a Teflon-lined stainless-steel autoclave (30 mL capacity). The autoclave was heated at 200 °C for 12 h and then allowed to cool to room temperature. The black products were separated magnetically and washed several times with ethanol and deionized water to eliminate organic and inorganic impurities before dispersing in

DMF for next experimentation.

3.2 Synthesis of Fe_3O_4@UiO-66 core-shell composites. 25 mg of Fe_3O_4 was added to 10 ml of DMF and ultrasonicated for 30 min. Then, the obtained dispersion was added to a DMF solution of MOF precursors, which contained 37.5 mg of $ZrCl_4$, 29 mg of NH_2-BDC and 8 mL of DMF. The resulting mixture was placed in a preheated oven at 80 °C for 12 h and then held at 100 °C for 24 h. After cooling down to room temperature, the resulting pale brown solid was magnetic separation and washed several times with ethanol and deionized water. The purified Fe_3O_4@UiO-66 core-shell composites were dispersed in phosphate buffer solution (PBS) and stored at 4 °C for further use. The core-shell composites with different morphology were synthesized according to the above procedure except altering the concentration of the precursors of UiO-66.

3.3 Synthesis of UiO-66 nanocrystals. UiO-66 nanocrystals were also prepared for comparison. Typically, $ZrCl_4$ (75 mg) and 2-aminoterephthalic acid (58 mg) were mixed with 18 mL DMF in a Teflon-lined stainless-steel autoclave (30 mL capacity). The autoclave was sealed and placed in an oven at 80 °C for 12 h and then held at 100 °C for 24 h. After cooling down to room temperature, the yellow precipitates were obtained by centrifugation. After being washed with DMF for three times, the solid was then washed with ethanol and collected by centrifugation at 10 000 rpm for 10 min. Finally, the UiO-66 nanocrystals were activated in vacuum at 60 °C for 12 h.

4. Drug loading and release

4.1 Drug loading. In a typical experiment, loading of DOX into Fe_3O_4@UiO-66 composites was accomplished by mixing 6 mL of different concentrations of DOX solution in phosphate buffer solution (PBS, 10 mM, pH 8.0) with 5 mg of Fe_3O_4@UiO-66. The mixture was placed on

the shaker for 24 h under dark conditions. Free DOX was removed by centrifugation and washing with PBS several times. The obtained Fe_3O_4@UiO-66-DOX was stored at 4 °C in the dark. The amount of free DOX in supernatant and washing solutions was determined by fluorescence spectrum (excitation at 480 nm, emission at 590 nm). The drug loading capacity (DLC) was calculated according to the following formula: DLC (wt%) = (weight of loaded DOX / total weight of loaded DOX and Fe_3O_4@UiO-66) × 100%.

4.2 Drug release. The drug release was studied by dispersing the Fe_3O_4@UiO-66-DOX sample into 8 mL of PBS at pH 4.0, 5.0, 6.0 and 7.4 and then shaking in dark. At different time point, 3.0 mL of supernatant was taken out after the dispersion was centifugated and replenished with an equal volume of fresh PBS. The amount of released DOX was quantified by fluorescence spectrum and the accumulated drug release (ADR) of DOX from Fe_3O_4@UiO-66-DOX was calculated according to the following formula: ADR (wt%) = $\{(8C_n + 3\sum_{i=1}^{n-1} C_i$)/weight of loaded DOX$\}$ × 100%, where C_n is the concentration of DOX in the supernatant at the time point of n.

5. Transverse relaxivity and T_2-weighted images

The samples with different Fe concentrations (0.00, 0.02, 0.04, 0.06, 0.08, 0.10 mmol/L) were prepared using Fe_3O_4@UiO-66 composites. Transverse relaxivity time (T_2) and T_2-weighted images of the samples were acquired using a MesoMR60 MRI system. The transverse relaxivity (r_2) of Fe_3O_4@UiO-66 was obtained by linear fitting of $1/T_2$ versus Fe concentration.

6. Cell and animal experiments

6.1 Cytotoxicity assays. HeLa cells (human cervical carcinoma cells) and 3T3 cells (3T3-Swiss albino) were cultured in RPMI-1640 medium containing 10% fetal bovine serum and 1% penicillin-streptomycin at 37 °C under 5% CO_2. The in vitro cytotoxicity of Fe_3O_4@UiO-66

composites was evaluated by MTT assays against HeLa cells. Briefly, Hell cells were plated in a 96-well plate with a density of 1 × 10^4 cells/well, and cultured for 24 h. Then, 20 μL of Fe_3O_4@UiO-66, Fe_3O_4@UiO-66-DOX or free DOX with various concentrations were added and incubated for 24 h. After the cell medium was replaced and washed with PBS, 10 μL of MTT (5 mg/mL) were added and incubated for another 4 h. Then, the MTT-formazan generated by live cells was dissolved in 120 μL of DMSO, and the absorbance at 490 nm of each well was monitored using a Synergy™2 Multi-Mode Microplate Reader. The cytotoxicity was estimated by the relative cell viability (%) compared with the untreated control cells.

6.2 Animal model. The adult Kunming mice (23-25 g) and female Balb/c nude mice were purchased from Beijing HFK bioscience Co., Ltd. (Beijing, China). All the animal procedures were approved by Tianjin Medical University Animal Care and Use Committee. The HeLa tumor models were generated by subcutaneous injection of 2×10^6 HeLa cells in 50 μL PBS into the inguina of each female Balb/c nude mouse. After 2~3 weeks, the mice was used for the following experiments when the tumor volume reached about 60~100 mm^3.

6.3 In vitro MR imaging. Hell cells were seeded into a 96-well plate at a density of 1 × 10^4 cells/well, and cultured for 24 h at 37 °C under 5% CO_2. Then, Fe_3O_4@UiO-66 with different concentrations of 25, 50, 100, 150 and 200 mg/L were added and incubated for 24 h. After that, the cells were washed with PBS for three times and then treated with trypsin. The cells containing Fe_3O_4@UiO-66 were precipitated by centrifugation and then dispersed in 0.2% xanthan gum for in vitro MR imaging on a clinical 3.0 T GE Signa Excite MRI system.

6.4 In vivo MR imaging. In vivo MR imaging of Kunming mice or HeLa tumor-bearing mice was carried out on a clinical 3.0 T MRI system (GE Signa Excite). Typically, 400 μL of 5 mg/mL

Fe_3O_4@UiO-66 solution in PBS (24 mg Fe/kg) was injected by tail vein into the Kunming mice or HeLa tumor-bearing mice anesthetized with 4% chloral hydrate (6 mL/kg). T_2-weighted MR images of mice before and after injection at desired time intervals were obtained on the MR scanner equipped with a special animal coil using a T_2 propeller sequence (slice thickness = 2 mm, slice spacing = 0.5 mm, TR/TE = 2932/141 ms, FOV = 8×8 cm, matrix =256×160).

6.5 In vivo antitumor efficacy. The HeLa tumor-bearing mice were randomly divided into two groups (n = 2, each group) and then were intravenously injected into 200 μL of PBS and Fe_3O_4@UiO-66-DOX (5 mg/mL for Fe_3O_4@UiO-66), respectively. The photos of mice were recorded every day after the treatment. After 30 days, all the mice were sacrificed and the solid tumors were taken out to be measured and compared. Furthermore, the tumor development of the mice with the treatment of PBS or Fe_3O_4@UiO-66-DOX was monitored by MR imaging for 21 days to accurately evaluate the antitumor efficacy.

6.6 Biodistribution and toxicology studies. Twelve Kunming mice were divided into four groups (n = 3, each group). Three groups were intravenously injected with 400 μL of 5 mg/mL Fe_3O_4@UiO-66 and sacrificed at certain time points after injection for 1, 7 or 30 days. Another group of mice without injecting Fe_3O_4@UiO-66 were scarified as the control group. The body weight of all the mice was measured to explore the in vivo physiological influences of the Fe_3O_4@UiO-66 composites. The blood biochemical parameters were measured in the clinical laboratory of Tianjin Medical University General Hospital. Major organs including heart, liver, spleen, lung and kidney of all the mice were harvested and used for biodistribution analysis. For biodistribution analysis, the major organs of the mice in each group were separately solubilized by aqua regia for determination of Fe content by AAS and Zr content by ICP-MS.

References

1. F. Xu, C. Cheng, D.-X. Chen, H. Gu, ChemPhysChem, 2012, 13, 336.

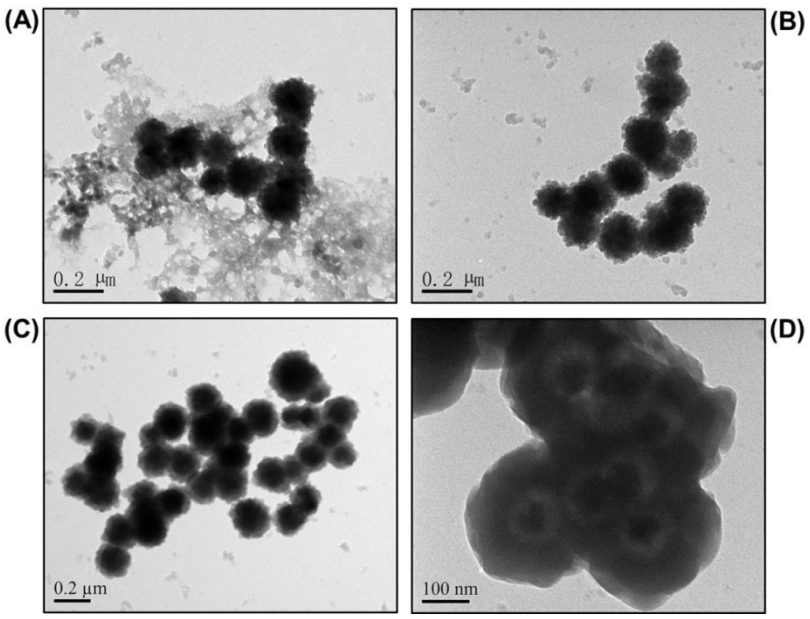

Fig. S1 TEM images of Fe_3O_4@UiO-66 composites synthesized by altering the UiO-66 precursor concentrations. $ZrCl_4$: NH_2-H_2BDC : DMF = 9.4 mg : 7.3 mg : 18 mL (A), 18.8 mg : 14.5 mg : 18 mL (B), 37.5 mg : 29 mg : 18 mL (C), 75 mg :58 mg : 18 mL (D).

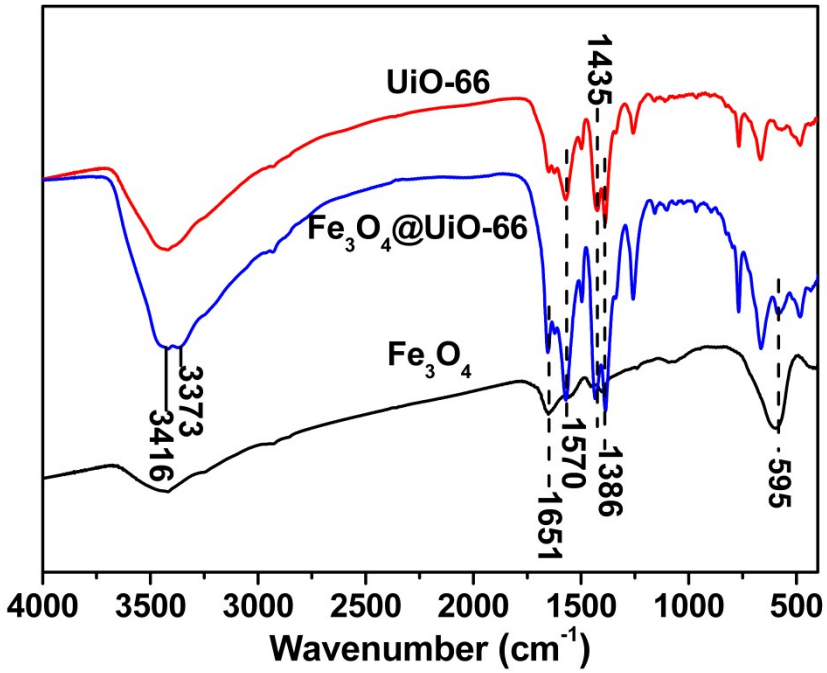

Fig. S2 FT-IR spectra of Fe_3O_4, UiO-66 and Fe_3O_4@UiO-66.

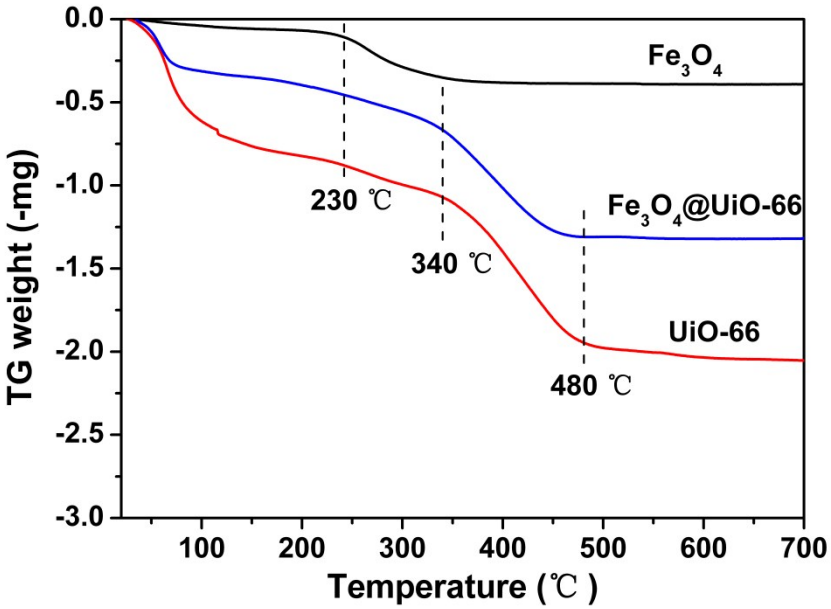

Fig. S3 Thermogravimetric analysis curves of Fe_3O_4, UiO-66 and Fe_3O_4@UiO-66.

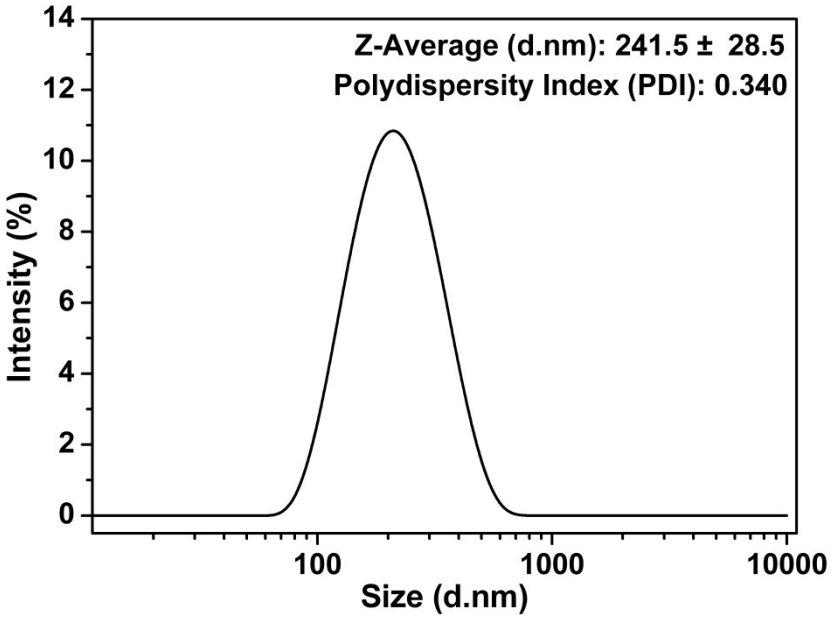

Fig. S4 DLS measured size distribution of Fe_3O_4@UiO-66 in PBS.

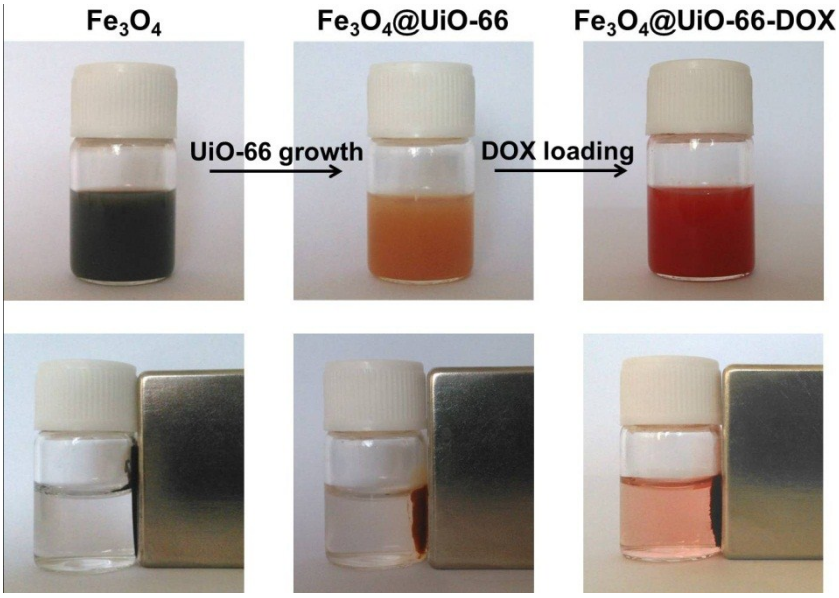

Fig. S5 Photos of Fe_3O_4, Fe_3O_4@UiO-66 and Fe_3O_4@UiO-66-DOX dispersion in the absence (upper) and presence (below) of a magnet field.

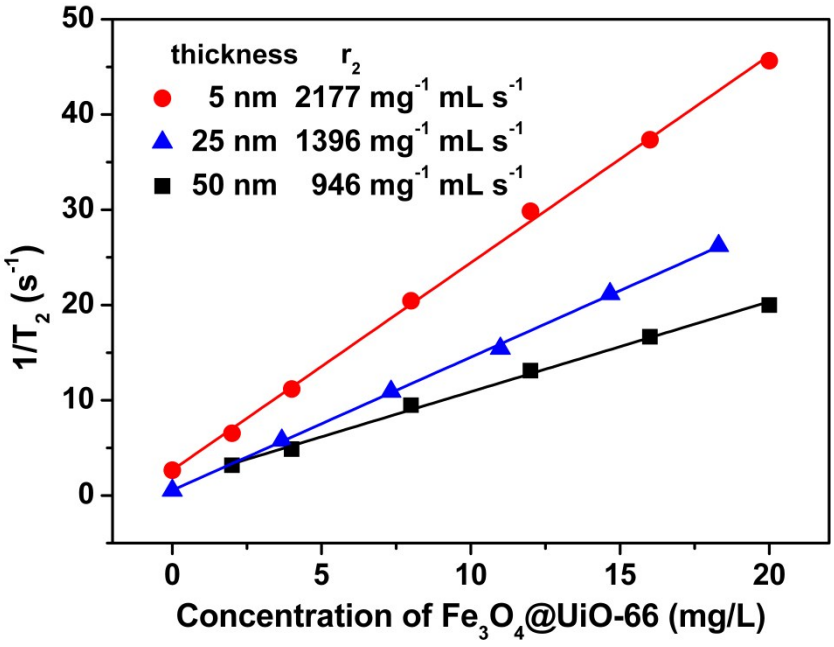

Fig. S6 The transverse relaxivities (r_2) of the Fe_3O_4@UiO-66 composites with different shell thickness of UiO-66.

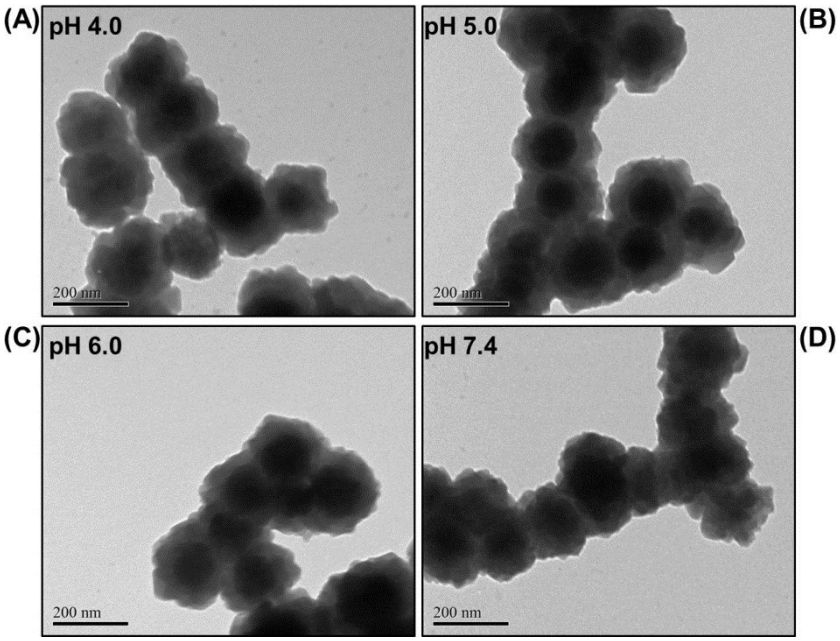

Fig. S7 TEM images of Fe_3O_4@UiO-66 composites after immersion in different pH solutions for one week.

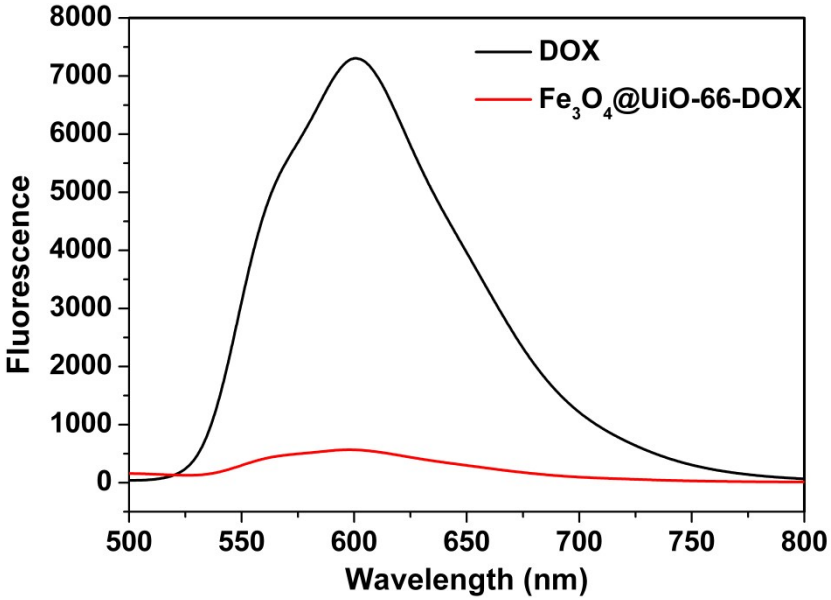

Fig. S8 Fluorescence spectra of free DOX and Fe_3O_4@UiO-66-DOX at the same DOX concentration of 0.20 mg/L.

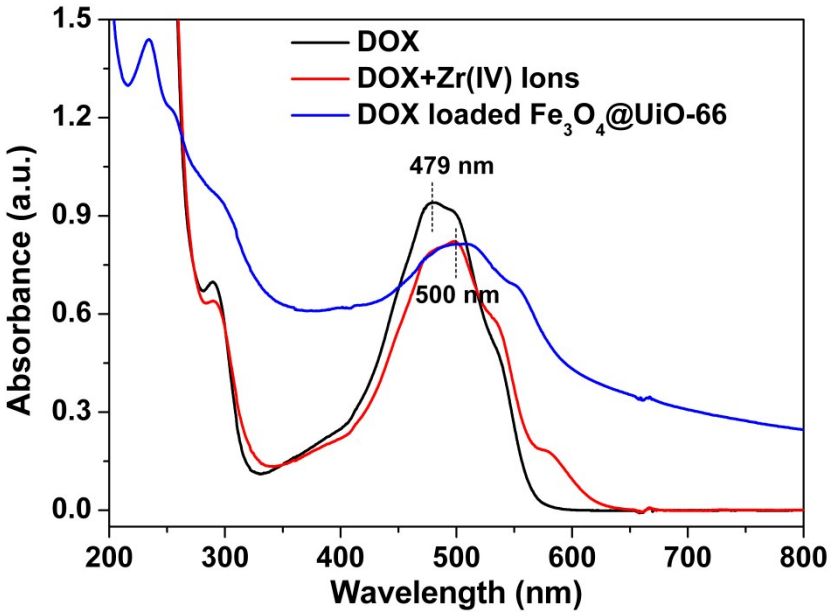

Fig. S9 UV-vis spectra of DOX solution, DOX and Zr(IV) mixed solution, DOX loaded Fe_3O_4@UiO-66 solution ([DOX]=0.04 g/L). DOX and Zr(IV) mixed solution was prepared by adding 50 μL of 0.6 mg/mL Zr(IV) aqueous solution to 1 mL 0.04 mg/mL DOX solution.

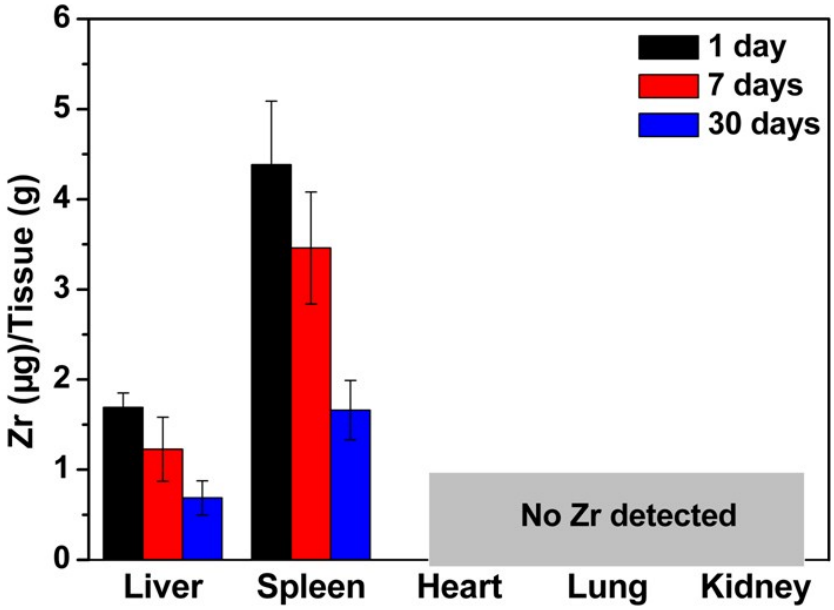

Fig. S10 Time-dependent biodistribution of Zr in various organs of mice.

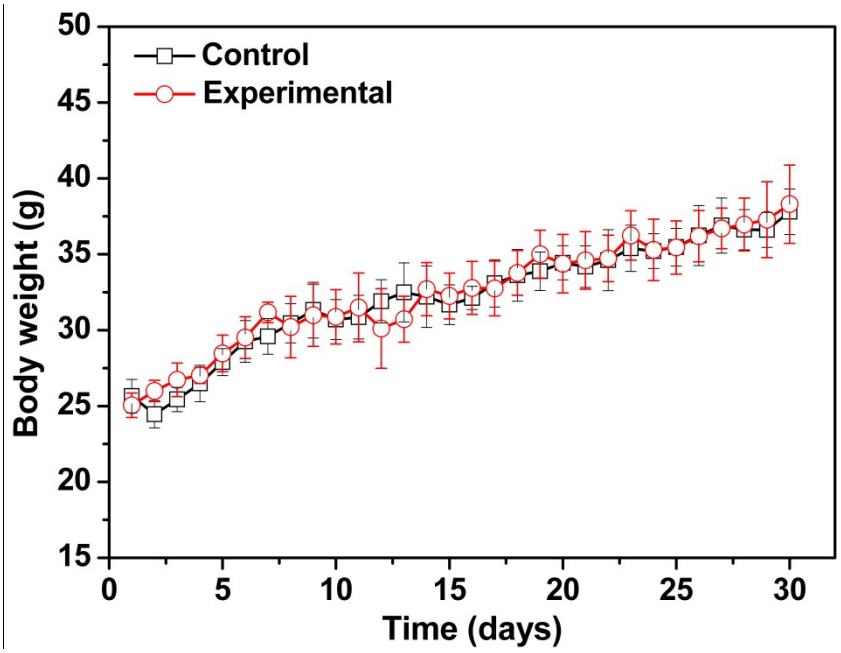

Fig. S11 Body weights of the control group and the experimental group treated with Fe_3O_4@UiO-66.

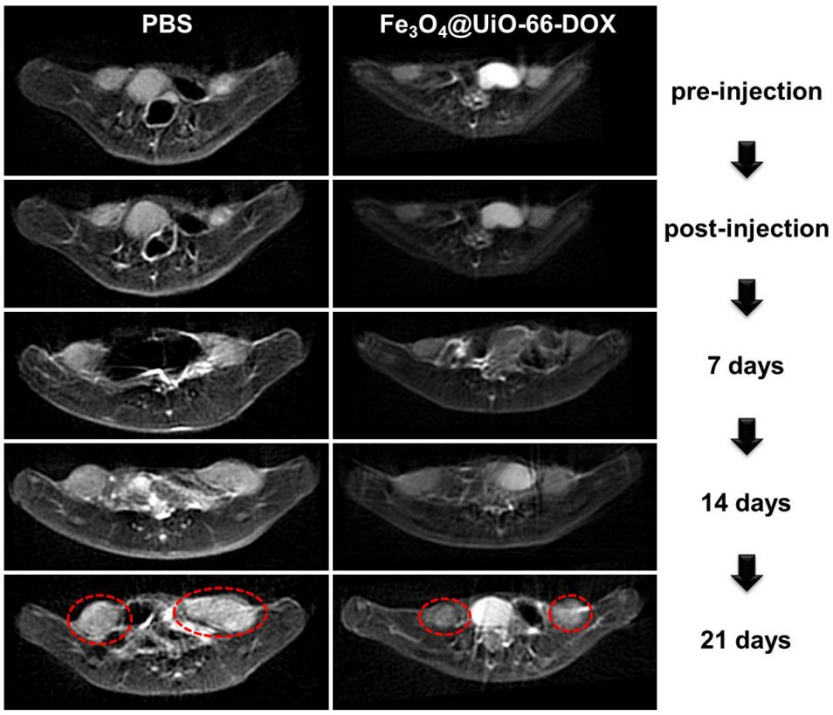

Fig. S12 MR images of HeLa-tumor bearing mice pre-injection and post-injection of PBS or Fe_3O_4@UiO-66-DOX at different time points (7 days, 14 days, and 21 days).

Table S1. Porosity properties of UiO-66 and Fe_3O_4@UiO-66.

sample	S_{BET} (m^2 g^{-1})	V_{total}[a] (cm^3 g^{-1})	D_{pore}[b] (nm)
UiO-66	702.88	0.44	4.8
Fe_3O_4@UiO-66	149.75	0.21	3.5

[a] V_{total} was measured at $P/P_0 = 0.99$.
[b] D_{pore} was calculated using Barrett-Joyner-Halenda (BJH) method.

Table S2. The r_2 and DOX loading capacity of Fe_3O_4@UiO-66 composites with different UiO-66 shell thickness.

UiO-66 shell thickness	5 nm	25 nm	50 nm
r_2 (mg^{-1} mL s^{-1})	2177	1396	946
Loading capacity (%)	23.4	66.3	85.5